



Original Article

# Production of Scalar Unparticle Pairs in Electron-positron Collisions

Dao Thi Le Thuy<sup>1</sup>, Le Nhu Thuc<sup>1,\*</sup>, Nguyen Quoc Hoan<sup>2</sup>

<sup>1</sup>Hanoi National University of Education, 136 Xuan Thuy, Cau Giay, Hanoi, Vietnam

<sup>2</sup>Thai Nguyen University - Ha Giang Campus, No.16 Group, Ha Giang, Tuyen Quang, Vietnam

Received 26<sup>th</sup> February 2026

Revised 25<sup>th</sup> March 2026; Accepted 28<sup>th</sup> April 2026

**Abstract:** In this work, we study the phenomenology of unparticle physics via the production of scalar unparticle pairs in electron-positron collisions ( $e^+e^- \rightarrow UU$ ) at high-energy colliders. Using numerical analysis methods, we perform a detailed investigation into the dependence of both the differential and total cross-sections on the characteristic model parameters ( $d_U, \Lambda_U$ ), the center-of-mass energy ( $\sqrt{s}$ ), and specifically the energy of the produced unparticles ( $E_U$ ). The numerical results reveal that the differential cross-section exhibits a strong angular dependence, peaking in directions parallel and anti-parallel to the incident beam. More importantly, the cross-section is significantly enhanced in the low  $E_U$  region and diminishes as  $E_U$  increases. This indicates that the energy loss of the initial  $e^+e^-$  beam is substantial in the low-energy regime, corresponding to the dominant emission of energetic unparticles. Regarding the total cross-section, our calculations show a rapid suppression as the center-of-mass energy  $\sqrt{s}$  and the energy scale  $\Lambda_U$  increase. Furthermore, the cross-section demonstrates critical sensitivity to the scaling dimension  $d_U$ ; as  $d_U$  increases from 1.1 to 1.9, the magnitude of the cross-section decreases by approximately 8 to 9 orders of magnitude. These findings suggest that experimental signatures of scalar unparticle production are most prominent in the low-energy regime and for models characterized by small scaling dimensions  $d_U$ .

**Keywords:**  $e^+e^-$  collisions, scalar unparticles,  $d_U, \Lambda_U$ , cross-section.

\* Corresponding author.

E-mail address: [thucln@hnue.edu.vn](mailto:thucln@hnue.edu.vn)

<https://doi.org/10.25073/2588-1124/vnumap.5118>

## 1. Introduction

The Standard Model (SM) of particle physics provides an extremely successful description of the fundamental particles and their interactions. Its predictions have been confirmed with high precision in numerous experiments. Nevertheless, the SM is widely believed to be incomplete, as it fails to address several fundamental open problems, such as the nature of dark matter, the origin of neutrino masses, and the hierarchy of energy scales. These unresolved issues strongly motivate the exploration of new physics beyond the Standard Model (BSM) [1].

Among various BSM frameworks, unparticle physics offers a distinctive and unconventional extension of the SM based on the concept of scale invariance. This idea was first introduced by Georgi, who proposed the existence of a hidden sector described by a conformal field theory with a nontrivial infrared fixed point, weakly coupled to the SM through higher-dimensional operators [2, 3]. Below a characteristic energy scale  $\Lambda_U$ , this hidden sector manifests itself as unparticles characterized by a non-integer scaling dimension  $d_U$ . As a consequence of scale invariance, unparticles do not possess a definite mass, leading to unusual phase-space properties and novel phenomenological signatures that differ markedly from those of ordinary particles.

Since its proposal, unparticle physics has been extensively investigated in a wide variety of theoretical and phenomenological contexts. Early studies primarily focused on the role of unparticles as virtual mediators in scattering processes, demonstrating that unparticle exchange can induce observable deviations from SM predictions in cross sections and angular distributions at high energies [4, 5]. These works laid the foundation for collider-oriented unparticle phenomenology and highlighted the sensitivity of precision observables to scale-invariant dynamics.

In recent years, interest in unparticle models has remained active, particularly in view of the absence of direct signals of new particles at the Large Hadron Collider. As a result, effective field theory approaches and indirect searches for new physics have gained increasing attention. Updated phenomenological analyses indicate that unparticle effects remain compatible with existing experimental constraints and can still lead to sizable contributions in high-energy and high-precision experiments for appropriate choices of the scaling dimension and coupling structure [6].

Electron–positron colliders provide an especially clean experimental environment for probing such nonstandard effects. Numerous studies have examined unparticle contributions to processes in  $e^+e^-$  collisions, including fermion pair production and missing-energy signatures, with particular emphasis on angular distributions and beam polarization effects [6, 7]. These investigations show that lepton colliders offer competitive and complementary sensitivity to unparticle parameters compared to hadron colliders.

Furthermore, the physics potential of future high-energy lepton colliders, such as the International Linear Collider and the Compact Linear Collider (CLIC), has renewed interest in unparticle phenomenology. With center-of-mass energies reaching the multi-TeV scale, these facilities are well suited to probe scale-invariant hidden sectors, where unparticle-induced deviations from the SM are expected to be enhanced [8–11]. In parallel, recent studies have also explored unparticle effects in precision scattering experiments, such as the MUonE experiment, illustrating that scale-invariant dynamics can leave measurable imprints even at low-energy but high-precision facilities [8].

Despite the extensive literature on unparticle physics, most existing works concentrate on scenarios in which unparticles appear either as virtual intermediate states or as single unparticle final states accompanied by Standard Model particles. By contrast, the direct production of unparticle pairs in  $e^+e^-$  collisions has not yet been systematically investigated, particularly for scalar unparticles. Such processes probe different aspects of unparticle dynamics and lead to characteristic missing-energy signatures that are distinct from those studied previously.

Motivated by the current status of research in this field, in this work we study the production of scalar unparticle pairs in electron–positron collisions within the framework of unparticle physics, analyzing the total and differential cross sections as functions of the unparticle scaling dimension, the unparticle energy scale, and the collider energy. Our results provide further insights into unparticle pair production and highlight the potential of future high-energy  $e^+e^-$  colliders to probe scale-invariant hidden sectors beyond the Standard Model.

## 2. The process $e^+e^- \rightarrow UU$

### 2.1. Scattering Amplitude

The production of a scalar unparticle pair in electron–positron collision proceeds only via the t- and u-channels through electron exchange, as shown in Fig. 1.

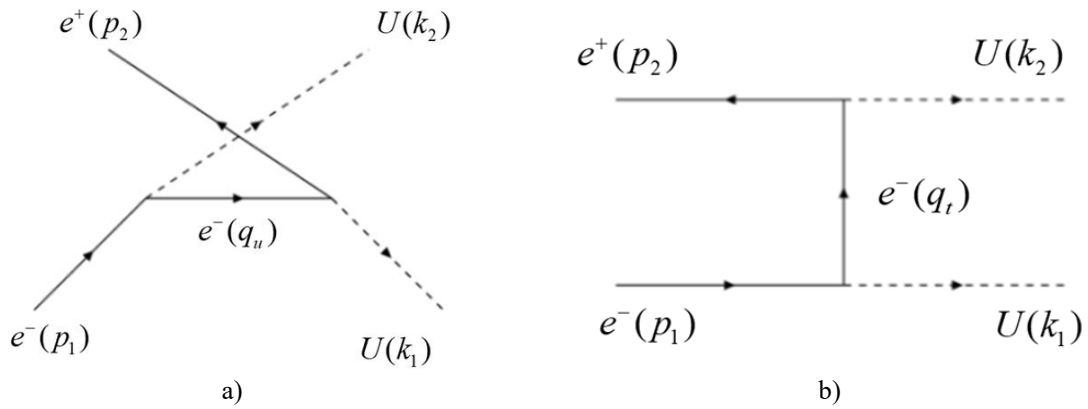


Figure 1. The Feynman diagram describing the process  $e^+e^- \rightarrow UU$ .

By applying the Feynman rules to Fig. 1, the corresponding scattering amplitude is obtained as

$$\begin{aligned}
 M_{fi} &= \frac{-i}{q_u^2 - m_e^2} \bar{v}(p_2, s_2) \left( i \frac{\lambda_0}{\Lambda_U^{d_U-1}} - \frac{\lambda_0}{\Lambda_U^{d_U-1}} \gamma_5 + \frac{\lambda_0}{\Lambda_U^{d_U}} \hat{k}_1 \right) \\
 &\times (\hat{q}_u + m_e) \left( i \frac{\lambda_0}{\Lambda_U^{d_U-1}} - \frac{\lambda_0}{\Lambda_U^{d_U-1}} \gamma_5 + \frac{\lambda_0}{\Lambda_U^{d_U}} \hat{k}_2 \right) u(p_1, s_1) \\
 &+ \frac{-i}{q_t^2 - m_e^2} \bar{v}(p_2, s_2) \left( i \frac{\lambda_0}{\Lambda_U^{d_U-1}} - \frac{\lambda_0}{\Lambda_U^{d_U-1}} \gamma_5 + \frac{\lambda_0}{\Lambda_U^{d_U}} \hat{k}_2 \right) \\
 &\times (\hat{q}_u + m_e) \left( i \frac{\lambda_0}{\Lambda_U^{d_U-1}} - \frac{\lambda_0}{\Lambda_U^{d_U-1}} \gamma_5 + \frac{\lambda_0}{\Lambda_U^{d_U}} \hat{k}_1 \right) u(p_1, s_1). \tag{1}
 \end{aligned}$$

### 2.2. Cross-section Formula

From equations (2.1), we calculate and obtain the square of the scattering amplitude of the  $e^+e^- \rightarrow UU$  process when the  $e^+, e^-$  beams are unpolarized. In the center-of-mass reference frame with

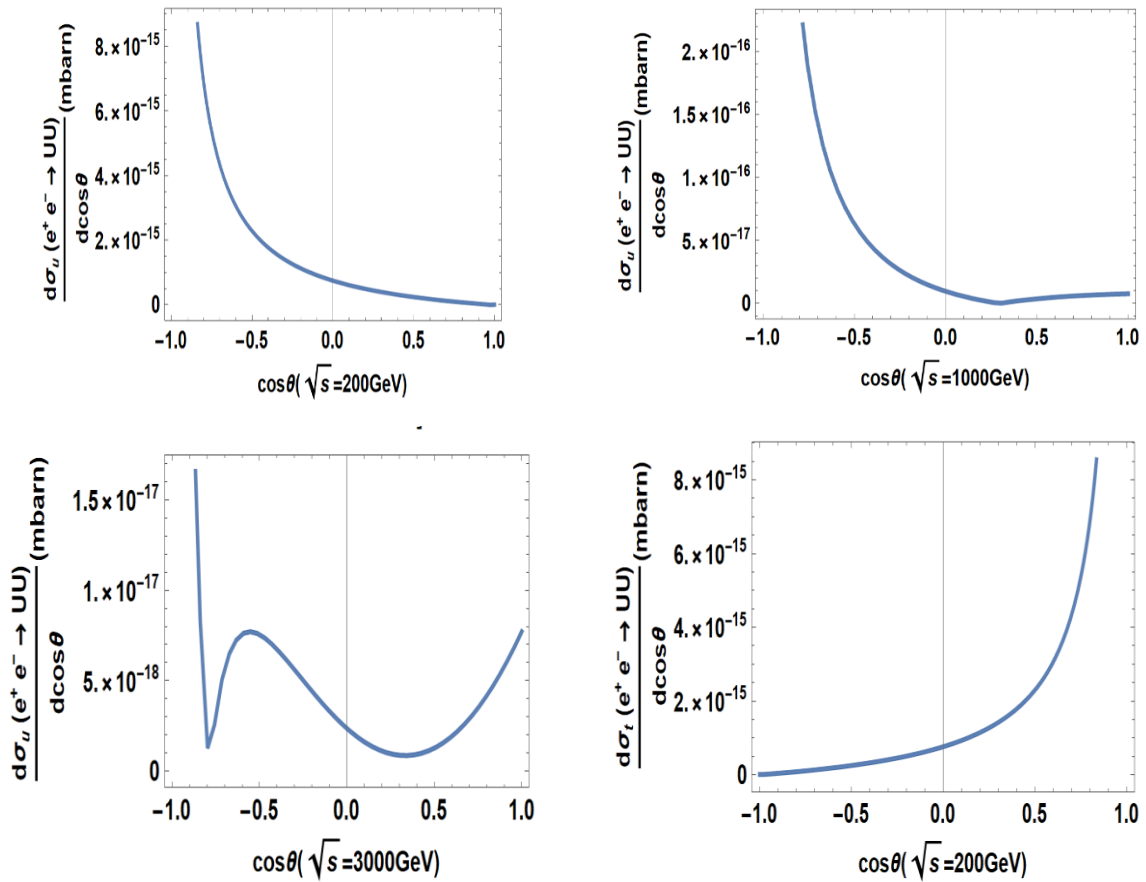
$p_1^\mu(E_1, \vec{p})$ ,  $p_2^\mu(E_2, -\vec{p})$ ,  $k_1^\mu(E_3, \vec{k})$ ,  $k_2^\mu(E_4, -\vec{k})$ ,  $E_1 + E_2 = E_3 + E_4 = \sqrt{s}$ , we calculate the DCS and the TCS according to the formula:

$$\frac{d\sigma}{d\Omega} = \frac{1}{64\pi^2 s} \frac{|\vec{k}|}{|\vec{p}|} |M_{fi}|^2, \quad (2)$$

where  $d\Omega = d\cos\theta d\varphi$ .

### 3. Results and Discussion

Numerical calculations and plots of the differential scattering cross section (DCS),  $\frac{d\sigma}{d\cos\theta}$ , as a function of the cosine of the scattering angle ( $\cos\theta$ ) are performed using *Mathematica* for the u-channel, the t-channel, and their combined contribution. The parameters are chosen as  $d_U = 1.7$ , and  $\Lambda_U = 1000\text{GeV}$ . The distributions are presented for several center-of-mass energies  $\sqrt{s}$ , corresponding to the low-, intermediate-, and high-energy regions, namely  $\sqrt{s} = 200\text{GeV}$ ,  $\sqrt{s} = 1000\text{GeV}$ , and  $\sqrt{s} = 3000\text{GeV}$ , respectively. The resulting plots are displayed in Fig. 2.



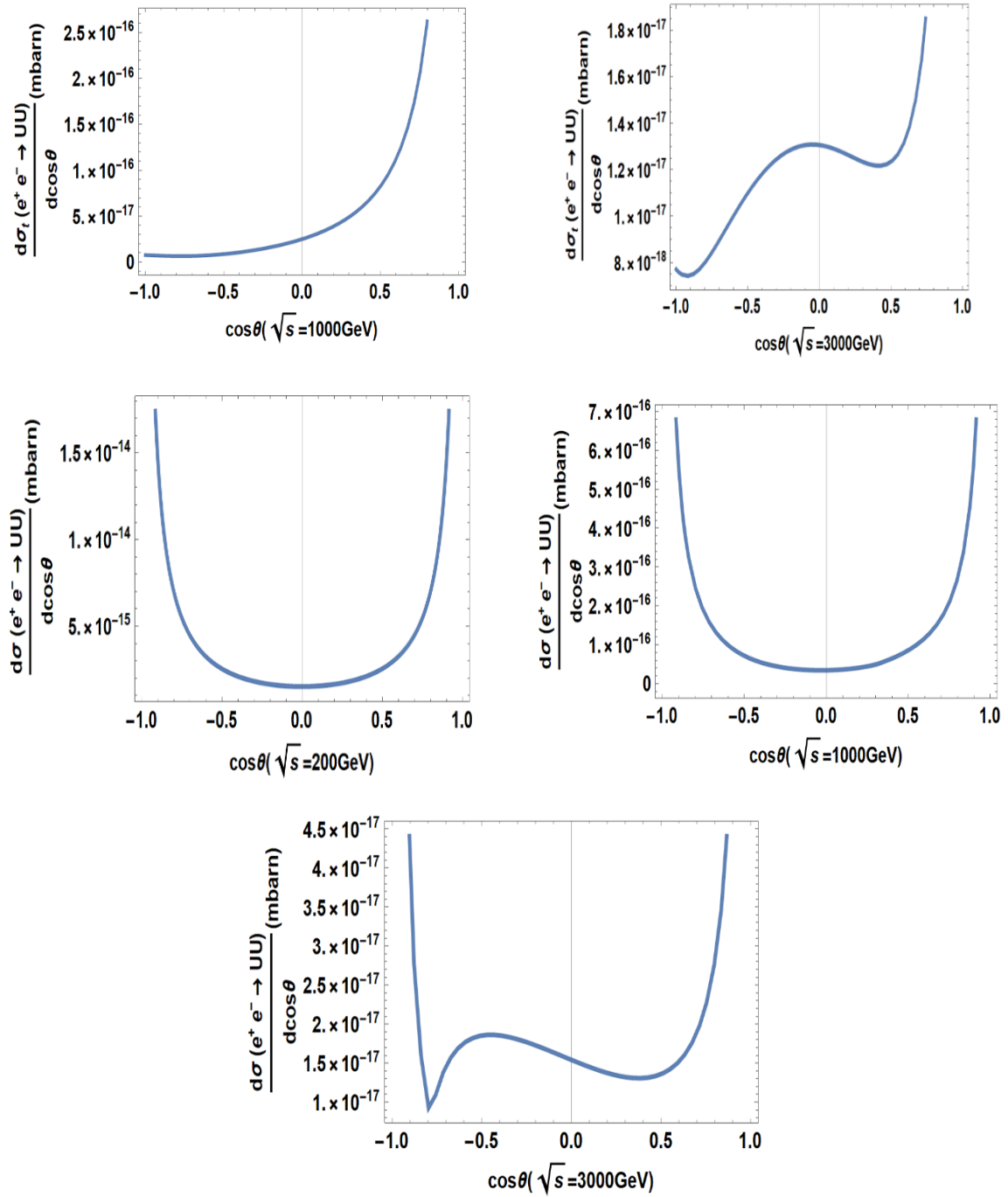


Figure 2. The differential cross section (DCS) as a function of  $\cos\theta$  for the process  $e^+e^- \rightarrow UU$ .

According to the plots in Fig. 2, it is observed that the DCS of the  $e^+e^- \rightarrow UU$  process depends significantly on the scattering angle. In all investigated cases, the value of  $\frac{d\sigma}{d\cos\theta}$  reaches its maximum

as  $\cos\theta \rightarrow \pm 1$ , corresponding to scattering in the same or opposite direction as the incident  $e^+, e^-$  beams. Meanwhile, the minimum values appear in the central region where  $\cos\theta \approx 0$ , which corresponds to the direction perpendicular to the original incident beam.

The maximum values of  $\frac{d\sigma}{d\cos\theta}$ , accounting for both  $u$  and  $t$  channels, are approximately:

$$1.8 \times 10^{-14} \text{ mb at } \sqrt{s} = 200 \text{ GeV}.$$

$$7 \times 10^{-16} \text{ mb at } \sqrt{s} = 1000 \text{ GeV}.$$

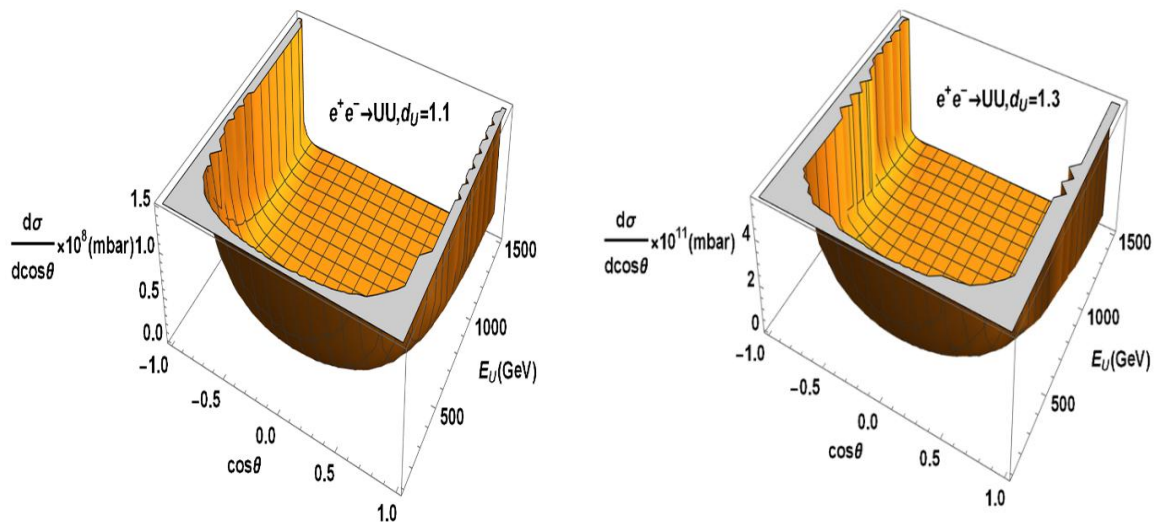
$$4.5 \times 10^{-17} \text{ mb at } \sqrt{s} = 3000 \text{ GeV}.$$

The minimum DCS values for both  $u$  and  $t$  channels at the corresponding center-of-mass energies are approximately  $3 \times 10^{-15} \text{ mb}$ ,  $8 \times 10^{-17} \text{ mb}$ , and  $1.1 \times 10^{-17} \text{ mb}$ . The plots demonstrate that the  $\frac{d\sigma}{d\cos\theta}$  for the  $e^+e^- \rightarrow UU$  process across both  $u$  and  $t$  channels increases sharply as  $\cos\theta \rightarrow \pm 1$ .

Fig. 3 describes the dependence of the DCS on  $\cos\theta$  and the energy  $E_U$  of the produced scalar unparticles with values  $d_U = 1.1, 1.3, 1.5, 1.7, 1.9$ . From Fig. 3, we have the following observations:

First, for a given produced unparticle scalar unparticles energy  $E_U$ , the DCS increases significantly as  $\cos\theta \rightarrow \pm 1$ , i.e., when the scattering angle approaches directions near-parallel and anti-parallel to the incident beam. Conversely, the DCS reaches its minimum value in the central angular region where  $\cos\theta \approx 0$ .

Second, at a fixed scattering angle, as the energy  $E_U$  of the produced unparticle scalar beam increases, the DCS decreases correspondingly. In other words, the DCS is only enhanced in the low-energy region, whereas at high energies, the probability of unparticle scalar pair production is strongly suppressed. Thus, the capability for unparticle pair production in the low-energy region is much greater than in the high-energy region.



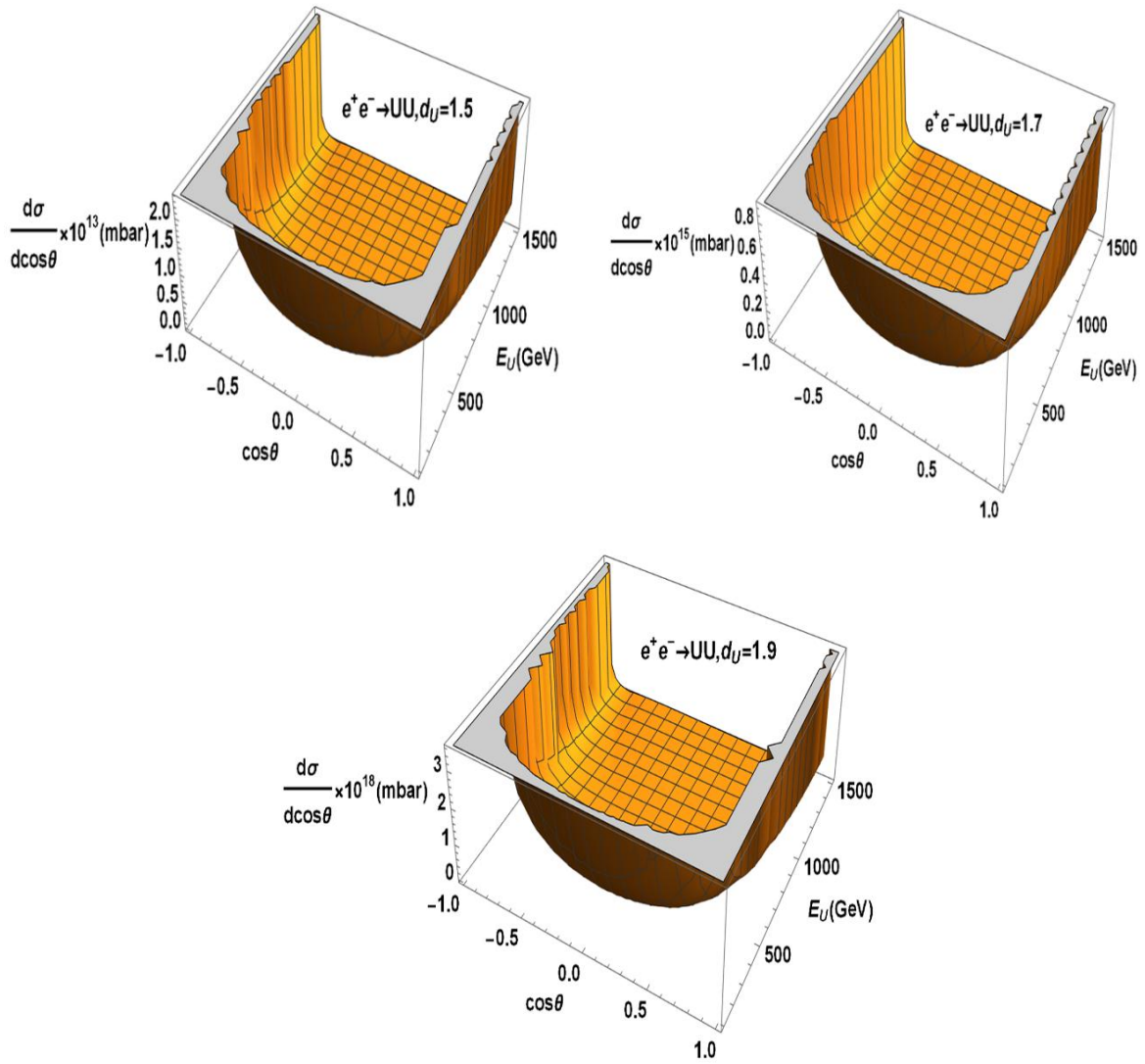


Figure 3. The DCS as a function of  $\cos\theta$  and the energy  $E_U$  of the scalar unparticle beam.

Third, as the scaling dimension parameter  $d_U$  increases, the DCS with respect to the scattering angle decreases significantly across the entire investigated range of angles and energy  $E_U$ . This decrease occurs simultaneously while the distribution shape relative to  $\cos\theta$  is nearly preserved, indicating that  $d_U$  primarily controls the absolute magnitude of the DCS with respect to the scattering angle.

In the numerical investigation of the total cross-section (TCS), we adopt the parameter set  $d_U = 1.1, 1.3, 1.5, 1.7, 1.9$  and  $\Lambda_U = 1000 \text{ GeV}$ , with the center-of-mass energy satisfying  $\sqrt{s} \leq 3000 \text{ GeV}$ . The resulting dependencies are illustrated in Fig. 4 as follows:

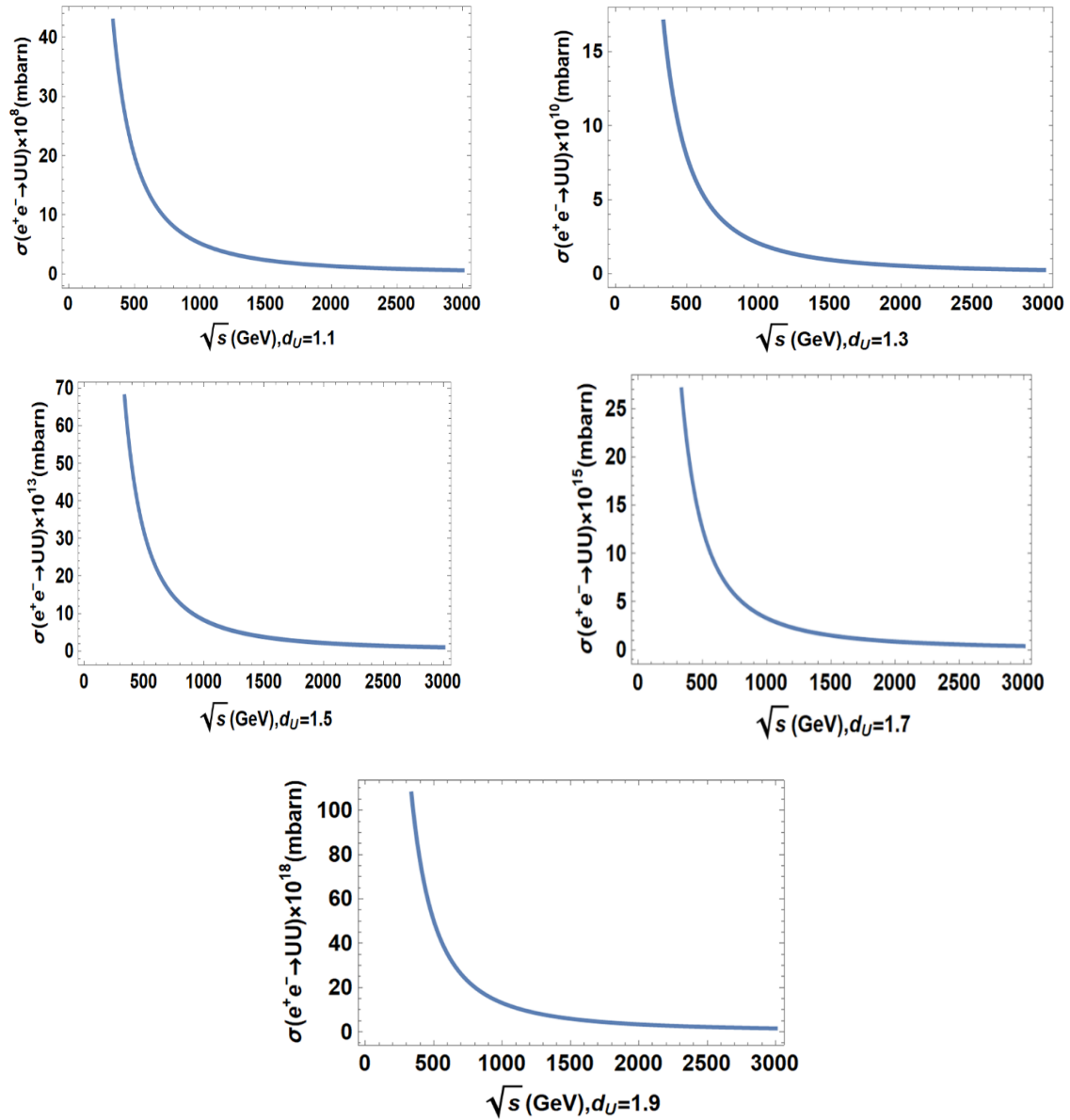


Figure 4. The dependence of the TCS on the center-of-mass energy  $\sqrt{s}$  for the process  $e^+e^- \rightarrow UU$ .

From the plots illustrating the dependence of the TCS on the center-of-mass energy  $\sqrt{s}$  for various scaling dimension values  $d_U = 1.1, 1.3, 1.5, 1.7, 1.9$ , several key observations emerge.

For a fixed value of  $d_U$ , the TCS reaches its maximum in the low-energy region of the incident beam. As the center-of-mass energy  $\sqrt{s}$  increases, the TCS decreases rapidly through the low-to-intermediate energy range, before declining more gradually toward very small values in the high-energy regime (at the TeV scale). This behavior indicates that the production of scalar unparticles is significantly suppressed as the center-of-mass energy  $\sqrt{s}$  rises.

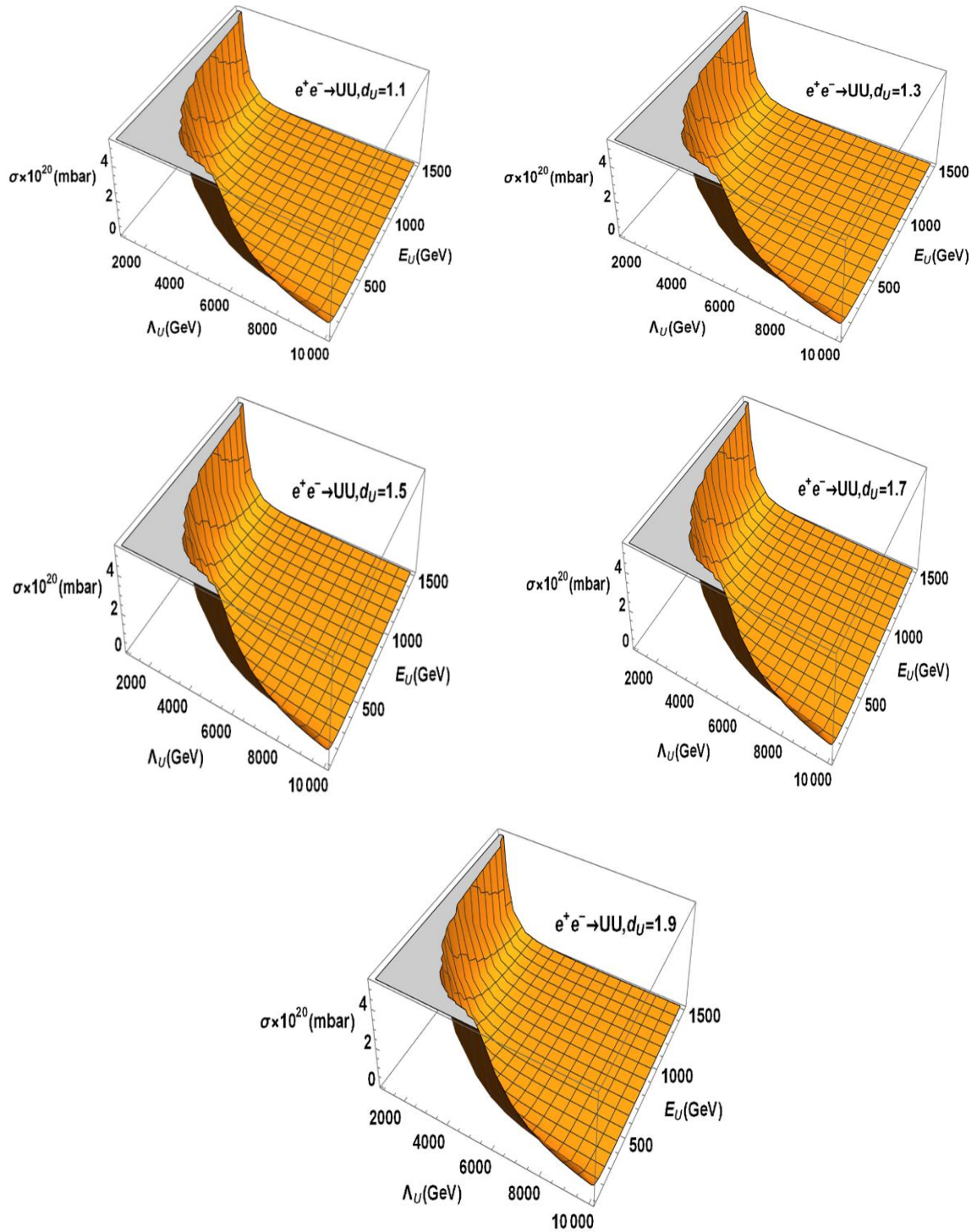


Figure 5. The dependence of the TCS on the unparticle energy  $E_U$  and the energy scale  $\Lambda_U$  for the  $e^+e^- \rightarrow UU$  process.

Furthermore, at a constant center-of-mass energy  $\sqrt{s}$ , the TCS exhibits a marked decrease as the scaling dimension  $d_U$  increases. Specifically, the case with  $d_U = 1.1$  yields the highest TCS values, whereas  $d_U = 1.9$  results in the lowest values among the selected parameters. In the investigated energy range, for  $d_U = 1.1$ , the TCS is approximately  $4 \times 10^{-9} mb$  at  $\sqrt{s} = 200 GeV$  and roughly  $2 \times 10^{-10} mb$  at  $\sqrt{s} = 3000 GeV$ . In contrast, for  $d_U = 1.9$ , the TCS values drop to approximately  $10^{-17} mb$  at  $\sqrt{s} = 200 GeV$  and  $2 \times 10^{-18} mb$  at  $\sqrt{s} = 3000 GeV$ .

Consequently, the scalar unparticle production effect is particularly pronounced at low energies for smaller  $d_U$  values. As  $d_U$  increases from 1.1 to 1.9, the TCS diminishes by approximately 8 to 9 orders of magnitude. Although both cases result in minimal cross-sections at high energies, the  $d_U = 1.1$  case remains notably more dominant. These findings reflect the fact that the production of scalar unparticles in  $e^+e^-$  collisions is strongly enhanced as  $d_U$  decreases.

The numerical results in Fig. 5, which illustrate the dependence of the TCS on the energy scale  $\Lambda_U$  of the unparticle physics model and the energy  $E_U$  of the produced scalar unparticles for  $d_U = 1.1, 1.3, 1.5, 1.7, 1.9$ , reveal that the TCS is strongly sensitive to  $\Lambda_U$ ,  $E_U$ , and the scaling dimension  $d_U$ .

Specifically, the TCS decreases rapidly as the energy scale  $\Lambda_U$  increases, reflecting a significant suppression of scalar unparticle production effects at higher energy scales. Simultaneously, the TCS attains higher values in the low- $E_U$  region and gradually diminishes as  $E_U$  rises, suggesting that the emission of scalar unparticles is favored at lower energies.

A comparison across different values of  $d_U$  further demonstrates that as  $d_U$  increases from 1.1 to 1.9, the magnitude of the TCS decreases markedly throughout the entire investigated range. Consequently, smaller  $d_U$  values lead to the most pronounced scalar unparticle production effects. These findings imply that high-energy collider experiments will exhibit higher sensitivity to unparticle physics models characterized by low scaling dimensions  $d_U$  and energy scales  $\Lambda_U$  situated in the TeV range.

#### 4. Conclusion

We first emphasize the experimental limitations of the direct measurement of the  $e^+e^- \rightarrow UU$  process. Since unparticles are expected to interact very weakly with Standard Model particles [2], they traverse the detector without leaving observable signals. As a result, the final state consisting of two unparticles is completely invisible, making direct detection infeasible and rendering this study primarily theoretical.

In practice, such invisible final states are probed via missing energy signatures, for instance through initial state radiation processes like  $e^+e^- \rightarrow \gamma + E$  [12, 13], where a detectable photon recoils against missing energy. Similar strategies have been employed in LEP measurements of single-photon events,

placing constraints on unparticle physics. Therefore, although the  $e^+e^- \rightarrow UU$  channel cannot be observed directly, it provides a useful theoretical baseline for future phenomenological studies.

Based on the numerical calculations for the scalar unparticle pair production process  $e^+e^- \rightarrow UU$ , we observe several distinctive features. Regarding the scattering direction, the differential cross-section exhibits a strong angular dependence, maximizing in directions parallel and anti-parallel to the incident beam while reaching its minimum in the transverse direction, indicating that particle production is predominantly aligned with the collision axis. In terms of the center-of-mass energy  $\sqrt{s}$ , the total cross-section peaks in the low-energy regime and decreases rapidly as  $\sqrt{s}$  increases, eventually approaching negligible values at the TeV scale. Concurrently, an analysis of the energy  $E_U$  of the produced scalar unparticles reveals that the cross-section is enhanced in the low- $E_U$  region and diminishes as  $E_U$  rises; this demonstrates that the energy loss (missing energy) of the initial  $e^+e^-$  beam is substantial in the low-energy regime, corresponding to a strong emission of unparticle currents. Finally, the magnitude of the cross-section proves to be critically sensitive to the model parameters  $d_U$  and  $\Lambda_U$ ; specifically, as  $d_U$  increases from 1.1 to 1.9, the cross-section drops drastically by approximately 8 to 9 orders of magnitude, and a similar suppression occurs with increasing energy scale  $\Lambda_U$ , confirming that scalar unparticle signatures are most observable in models characterized by small  $d_U$  and low  $\Lambda_U$ .

## References

- [1] K. Hikasa, CPT, Majorana Fermions, and Particle Physics Beyond the Standard Model, *Prog. Theor. Exp. Phys.*, 2024, pp. 08C101, <https://doi.org/10.1093/ptep/ptae081>.
- [2] H. Georgi, Unparticle Physics, *Phys. Rev. Lett.*, Vol. 98, 2007, pp. 221601, <https://doi.org/10.1103/physrevlett.98.221601>.
- [3] H. Georgi, Another Odd Thing About Unparticle Physics, *Phys. Lett. B*, Vol. 650, 2007, pp. 275.
- [4] K. Cheung, W. Y. Keung, T. C. Yuan, Collider Phenomenology of Unparticle Physics, *Phys. Rev. D*, Vol. 76, 2007, pp. 055003.
- [5] T. M. Aliev, A. S. Cornell, N. Gaur, Lepton Pair Production in Unparticle Physics, *JHEP*, Vol. 07, 2007, pp. 072.
- [6] L. N. Thuc, D. T. L. Thuy, The Scalar Unparticle Production from the Collision Process  $\gamma e^-$  in Unparticle Physics, *VNU Journal of Science: Mathematics–Physics*, Vol. 36, No. 1, 2020, pp. 7-12.
- [7] D. T. L. Thuy, Phenomenology of Scalar Unparticle Production At Lepton Colliders, *Commun. Phys.*, Vol. 31, 2021, pp. 411.
- [8] D. N. Le, V. D. Le, D. T. Le, V. C. Le, Unparticle Effects at the MUonE Experiment, *Eur. Phys. J. C*, Vol. 83, 2023, pp. 1037.
- [9] S. Kumar, P. Poulou, Probing Unparticle Physics at Future Lepton Colliders, *Eur. Phys. J. C*, Vol. 80, 2023, pp. 168.
- [10] M. Rashed, Unparticle Effects in Fermion Pair Production at ILC and CLIC, *Int. J. Mod. Phys. A*, Vol. 36, 2021, pp. 2150123.
- [11] CLIC and CLICdp Collaborations, The Compact Linear Collider (CLIC) – Summary Report, CERN Yellow Reports: Monographs, 005-M, Published by CERN, CH-1211 Geneva 23, Switzerland, Vol. 2, 2018, <https://doi.org/10.23731/CYRM-2018-002>.
- [12] K. Cheung, W. Y. Keung, T. C. Yuan, Collider Signals of Unparticle Physics, *Phys. Rev. Lett.*, Vol. 99, 2007, pp. 051803.
- [13] P. J. Fox, A. Rajaraman, Y. Shirman, Bounds on Unparticles from the LEP, *Phys. Rev. D*, Vol. 76, 2007, pp. 075004.